

Contents list available at CBIORE journal website

Remarkable Energy Development

Journal homepage: https://ijred.cbiore.id



Research Article

Experimental investigation of the cooling effect in an autonomousorienting conventional solar still

Oussama Drissi Maliani* , Khalid Guissi , Reda Errais , El Houssain Baali , Younes El Fellah

Renewable Energies Laboratory, Energy and Farm Machinery Department – Hassan II Institute of Agronomy and Veterinary Medicine – Madinat Al Irfane, B.P. 6202. Rabat – Morocco

Abstract. This study aims to assess the cooling effect of the condensing glass cover in a high-temperature conventional solar still (CSS) that dynamically operates, continuously changing its orientation to track the sun from sunrise to sunset. The solar distiller was integrated with a 2-axis solar tracking system assisted by a parabolic trough concentrator (PTC). Throughout the day, the CSS adjusts its orientation while the PTC maintains constant focus on the absorber at the bottom of the still, thereby enhancing the evaporation processes. Simultaneously, the planned cooling processes of the top glass cover are in operation. The impact of two different cooling techniques was investigated. The first one consisted of flowing cooling water over the condensing glass of the PTC-CSS, while the second technique aimed to submerge the entire condensing cover using a modified basin. The analysis revealed positive impact regarding the CSS performance with condensing surface cooling compared to the tubular solar still (TSS). Flowing water had a limited effect on reducing the glass cover's temperature, resulting in only a 2°C decrease. Nonetheless, this yielded 4050 ml/day, marking a 12.16% increase. The second technique widened the water–glass temperature difference, leading to an improvement in productivity up to 6120 ml/day, which is 69.48% higher than that achieved with no cooling. Overall efficiency of the device can be assessed as moderate to low, owing to the high temperature of the condensing cover that continues to be the most significant constraint for the CSS associated with PTC.

Keywords: solar still, cooling, desalination, distillation, solar tracker, parabolic trough concentrator



@ The author(s). Published by CBIORE. This is an open access article under the CC BY-SA license (http://creativecommons.org/licenses/by-sa/4.0/).

Received: 6th Oct 2024; Revised: 27th May 2025; Accepted: 25th June 2025; Available online: 20th July 2025

1. Introduction

The continuous increase in need for drinkable water is becoming a crucial problem and a threatening issue for many countries in different parts of the world. According to a United Nations report, 2.2 billion people still lacked safely managed drinking water in 2022 (UN DESA, 2023). Varieties of factors are at the origin of this situation, including population growth, industrialization and global warming.

In response to these challenges, scientists have been exploring innovative solutions to provide drinkable water without risking contamination or harming the environment. One effective approach is the desalination of seawater, particularly through the use of solar desalination techniques. By optimizing the efficiency of solar stills, which harness renewable solar energy, this method promotes access to clean water, a critical component of Sustainable Development Goal 6, while enhancing energy efficiency, thus contributing to Goal 7. The improved productivity of solar stills not only increases water availability but also reduces reliance on energy-intensive desalination processes, minimizing carbon emissions and supporting climate action initiatives outlined in Goal 13.

Recent advancements in solar desalination have led to the development of innovative solutions to address the challenges of sustainable freshwater production. Among these

advancements, nanofluids stand out as a promising technology for enhancing the efficiency of traditional solar systems. Due to their exceptional thermophysical properties, nanofluids improve heat transfer and overcome the limitations of solar stills, significantly boosting performance(Singh et al., 2024). In parallel, the integration of phase change materials (PCM) into solar desalination systems has demonstrated significant potential for storing excess thermal energy. These materials enable stable freshwater production even in the absence of direct solar radiation, while maximizing the utilization of renewable energy resources (Kumar et al., 2022). Furthermore, solar-assisted heat pumps have emerged as a sustainable solution for thermal desalination. Studies show that integrating transcritical CO2 heat pumps into desalination processes can reduce electrical consumption to 3.2 kWh/m³ when simultaneous potable water production and cooling energy are considered, surpassing the performance of traditional reverse osmosis systems (Petersen et al., 2024). These innovations underscore the growing importance of multidisciplinary approaches to addressing the challenges of freshwater production in the context of resource

Various desalination techniques have been implemented worldwide, relying on diverse technologies such as distillation,

^{*} Corresponding author Email: o.drissi@iav.ac.ma (O.D.Maliani)

reverse osmosis, centrifugation, compressive steam, and electrodialysis (Alrubaiea *et al.*, 2021). Among these, conventional solar stills are among the oldest devices used for water distillation. These stills benefit from solar thermal energy to desalinate saline or brackish water, ultimately producing pure drinkable water. Their operational principle is straightforward: saline water inside the still is heated by absorbing solar radiant heat, causing it to evaporate; the produced water vapor condenses on the cooler inner surface of the cover, and the condensed water trickles down into a container.

A wide range of desalination processes have been developed and implemented worldwide, each relying on distinct technologies such as reverse osmosis, multi-stage flash distillation, electrodialysis, centrifugation, vapor compression, and solar-driven distillation (Varun Raj & Muthu Manokar, 2017). Among these, conventional solar stills are one of the oldest and most widely recognized devices for water desalination. These systems harness solar thermal energy to convert saline or brackish water into pure drinkable water through a simple yet effective process of evaporation and condensation. While more advanced technologies dominate industrial-scale desalination, conventional solar stills remain particularly valuable in rural and remote areas, where access to electricity and complex infrastructure is limited.

Conventional solar stills have garnered significant interest from researchers in the field of water desalination due to their numerous advantages, such as being cost-effective, requiring minimal maintenance, and being environmentally friendly. However, compared to other desalination processes, basin-type solar stills have historically suffered from low productivity and efficiency. This disadvantage can be attributed to two major constraints: (i) the low rejection of latent heat to the atmosphere and (ii) the difficulty of raising evaporation temperature without adversely affecting the condenser temperature, as heating, evaporation, and condensation occur in the same chamber (He & Yan, 2009).

One of the most attractive techniques used to improve the solar still productivity is the cooling of the glass cover(Cuce et al., 2021); indeed, on the inner surface of the glass cover, water vapor is condensed and releases its latent heat of vaporization. The heat energy absorbed by the glass cover reduces the temperature difference between basin water and glass cover, which contributes to the decrease of the natural circulation of air mass inside the still. On the other side, the natural convection with the atmosphere continues to reduce the heat energy gained by the glass cover from its inner surface. However, this heat transfer process remains very weak to keep a sufficient temperature difference between saline water and the glass cover, especially at low wind speeds. So, using a cooling process of the glass cover enlarges the gap between saline water's temperature and that of glass cover. This enhances the condensation rate and, consequently, improves the yield of the solar still.

For this purpose, many researchers have studied and used different methods of glass cover cooling like flowing cold water over the glass cover (Arunkumar *et al.*, 2015), using wet cloth (Fath & Ghazy, 2002), generating natural internal air flow under the thermosyphon effect (Rahmani *et al.*, 2015) and combining between free and forced convection flows (Hafs *et al.*, 2023). G.M. Ayoub *et al.* (2013) have investigated the effect of cover cooling using an external fan close to three different cover shapes of a modified still: (i) single-sloped, (ii) double-sloped cover and (iii) curved cover. The fan was placed at different locations on top or side of the still covers as well. It was concluded that the daily still productivity is enhanced by 54 to

62% with and without air flow, respectively. The straight side of the single-sloped cover was determined as the best location to place the fan. On the other hand, the cover cooling technique has no considerable impact on the yield of fresh water during the off-shine period as revealed by the experiments conducted by Srithar *et al.* (2016).

Solar stills can be classified into two major categories: active solar stills and passive solar stills. An experimental study conducted by Morad et al. (2015) on both passive and active double slope basin solar still with and without glass cover cooling has shown a noteworthy increment of still productivity when utilizing a process of glass cover cooling. The yield of both passive and active solar still was expanded from 6.38 to 7.8 L.m⁻ ².day⁻¹ and from 8.52 to 10.06 l.m⁻².day⁻¹ respectively. Shoeibi et al.(2022) conducted a comparative study of double-slope solar still, hemispherical solar still, and tubular solar still using Al₂O₃/water film cooling, employing CFD analysis. The study revealed that the water productivity of double-slope solar desalination, enhanced by nanofluids film cooling, is improved by about 4.8% compared with tubular solar desalination employing nanofluid film cooling. Also, it was found that the net CO₂ mitigation for double-slope solar desalination and tubular solar desalination was 14.08 tons and 13.44 tons, respectively.

Many research studies have shown the effectiveness of glass cover cooling to enhance still productivity (Le *et al.*, 2021). Nevertheless, if the cooling process has not been carried out efficiently, it may have a reverse effect because the presence of a water film can diminish the transmission of solar rays into the still. Also, it could neutralize the influence of wind speed susceptible to cool the glass cover and therefore reduce the still efficiency.

Besides spraying and flowing water on the glass cover, other researchers employed an alternative method to cool glass water, which involves creating a double glazing gap with the initial glass cover and allowing cool water to pass through it. Arunkumar *et al.* (Arunkumar *et al.*, 2013) have used this technique in their investigation on a tubular solar still with a double glass cover integrated with a compound parabolic concentrator. They found that the water cooling process used has enhanced the still productivity by 144% and the yield went from 2.05 1/day to 51/day. The gap was used also to force the circulation of air flow at constant rate of 4.5 m/s using air blower. Another improvement in the yield of 49% was noticed.

Furthermore, another group of researchers has used thermoelectric devices to enhance the productivity and the performance of a solar still. For example, Rahbar et al. (2016) have conducted an experimental study on the performance of an asymmetrical solar still utilizing a thermoelectric cooler (TEC). The findings showed that productivity was 3.2 times greater when the TEC was used. Thanks to the lower temperature of the glass cover, the solar still has started to produce fresh water earlier by 3 hours. Also, Al-Madhhachi and Gao (2017) have used the thermal energy of both the hot and cold sides of a thermoelectric module in order to develop an efficient thermoelectric water distillation system. The thermoelectric module used was based on the Peltier effect. Laboratory experiments carried out declared that the system produces an amount of distilled water equivalent to 0.678 L/m² over a period of 1 h. The corresponding electrical energy required for water production was about 0.0324 kWh.

In the same way, solar concentrators and solar collectors have shown promising outcomes when they were used as heat energy boosters to promote the water yield of diverse desalination units. Prado *et al.* (2016) have carried out the performance of a solar dish concentrator for desalting brackish

and saline water. Very high temperatures of 198 °C and 319 °C were reached by the absorber when volumes considered were 21.84 cm3 and 5.47 cm3 respectively. Using a solar air collector to increase water temperature and the temperature difference between evaporation and condensation surfaces is another enhancement technique of the solar still that was used by Azari et al. (2021) .Results revealed that the annual output energy and exergy of their modified still was 170% and 257% higher than the conventional one, respectively. Maliani et al. (2020) introduced a parabolic trough concentrator with a two-axis solar tracker integrated with a modified conventional solar still. Experiments conducted under a low ambient temperature (19-26°C) have shown that the innovative system proposed provided a quasi-constant of water exceeding 80 °C.

Continuous direct exposure of sunlight to the absorber of a solar still results in a significant rise in water temperature, thereby enhancing the evaporation process. However, this can affect the temperature of the condensing cover and minimize the driving force between the evaporation and condensation processes and, consequently, decrease the still productivity. Elashmawy (2017) has conducted an experimental investigation of a parabolic concentrator solar tracking system integrated with a tubular solar still. He observed that the difference in temperature between water and glass cover was only 2.5°C at most. Compared to other works where the same type of solar still was experimented without integrating it with a concentrator, the temperature difference (T_w-T_g) was widely great than this value and was often in the vicinity of 10°C. The same remarks were declared by Maliani et al. (2020) in their experimental investigation of a conventional solar still assisted parabolic trough concentrator (PTC). Authors have reported that when the glass cover temperature goes beyond the threshold of 60 °C, it remains nearly the same for all time intervals of the experiment. At the end, and after 10 hours of the experiment, the glass cover continued to keep a hightemperature value of 53°C. In comparison to other solar stills operating in the same ambient temperature, this glass cover temperature was never reached, and the maximum was approximately 40 °C, after 5 to 6 hours of operating time.

As depicted above, it is well known that the cooling surface of a solar still has a positive impact on its productivity. However, in a recent study conducted on a TSS integrated with a PTC assisted solar tracker, Elashmawy (2019) has revealed that tube cooling surface of PTC-TSS is a very critical and sensitive process and almost has a negative impact on the productivity and performance of the tubular solar stills. This conclusion still not verified for a CSS working under the same conditions, i.e.: solar still is integrated with parabolic trough concentrator, changes permanently its orientation to track the sun from sunrise to sunset, with the still absorber receiving directly and continuously the concentrated sun rays (heating, evaporation and condensation processes take place in the same chamber). Therefore, this work, as a continuation of the research initiated by Maliani et al. (2020), aims at revealing the cooling effect on the yield of a high temperature conventional solar still assisted by a parabolic trough concentrator equipped with a two-axes solar tracker.

2. Experimental setup and methodology

2.1. Geometrical description of the PTC-CSS

2.1.1. Basin description

The basin of the solar still described in this study consists of two primary components: a semi-cylindrical absorber created by

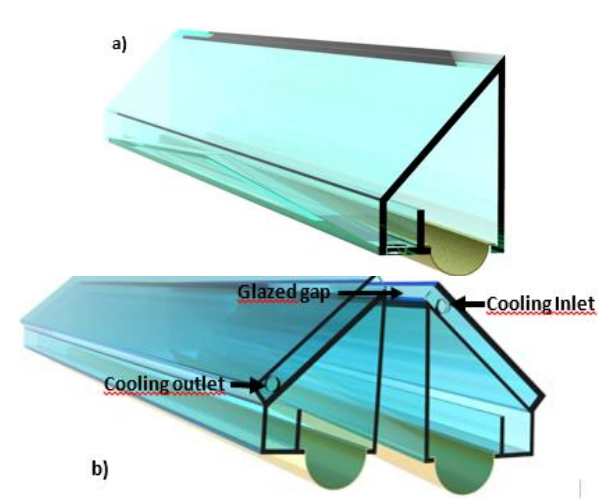


Fig. 1. (a) 3D view of the basic basin. (b) 3D view of the modified basin.

cutting a copper tube, measuring 1.8 meters in length and 0.05 meters in diameter, and a single-slope glass cover with internal dimensions of $1.80 \times 0.09 \times 0.17$ meters. The absorber and glass cover were sealed together using high thermal performance silicon caulking to prevent air infiltration and vapor leakage. The basin described was used in no cooling mode (case I) and cooling mode by flowing water over the condensation glass cover (case II). Then, it was modified to meet the requirement of the second cooling mode that of submerging the condensing glass cover by cooling water (case III). The modification made was creating a gap over the condensation glass cover using some pieces of glass. Two lateral orifices were used to allow the cooling water flow between the two glasses. The schematic view of the two versions of the basin is shown in Fig. 1.

An inclination of 60° relative to the horizontal was chosen to facilitate the smooth flow of condensed water, preventing excessive reflection of solar energy and the formation of large droplets. To enhance the thermal capacity of the still, copper was selected as the absorber material due to its superior thermal properties compared to glass and other metals. Accordingly, a copper tube measuring 0.05 meters in diameter and 1.80 meters in length was halved transversally to create the semi-cylindrical absorber. Given the elongated structure of the solar still basin, two gently sloping glass surfaces terminating in orifices were employed to collect condensed water efficiently. Additionally, a 4-centimeter-high glass barrier was inserted between the absorber and the two gentle glass slopes to prevent the mixing of distilled water with brackish water. Subsequently, the collected condensed water was stored in two graduated plastic bottles for subsequent measurements.

2.1.2. Concentrator description

The basin described previously was mounted onto an iron support, which was paired with a parabolic concentrator to create the PTC-CSS (Parabolic Trough Concentrator-Conventional Solar Still). The parabolic concentrator was built using a wooden frame and a rectangular, polished stainless steel sheet measuring 2 meters in length and 1 meter in width. The parabolic concentrator moves around its geometrical focus line in order to keep water in a horizontal position inside the still's basin while tracking the sun. Many calculations were made to set the parameters of the cylindro-parabolic reflector. Therefore, the focal length was chosen equal to the height of the curve of the parabola, and the arc length was almost equal to

Table 1
System design parameters of PTC-CSS

Item	Characteristic		
Basin still			
Shape	Single slope		
Dimensions (length ×weight×height)	$1.8 \text{ m} \times 0.09 \text{ m} \times 0.17 \text{ m}$		
Inclination angle	60°		
Glass thickness	4 mm		
Gap thickness(for the modified version of basin)	5 mm		
Absorber			
Dimensions (length× diameter)	$1.8 \text{ m} \times 0.05 \text{ m}$		
Thickness	1 mm		
Material	Copper		
PTC			
Reflector material	Polished stainless steel		
Reflectivity coefficient	80%		
Aperture area	2 m^2		
Focal length	0.22 m		
Aperture diameter	0.88 m		
Height of the curve	0.22 m		
Solar tracker	Automatic, 2-axis		

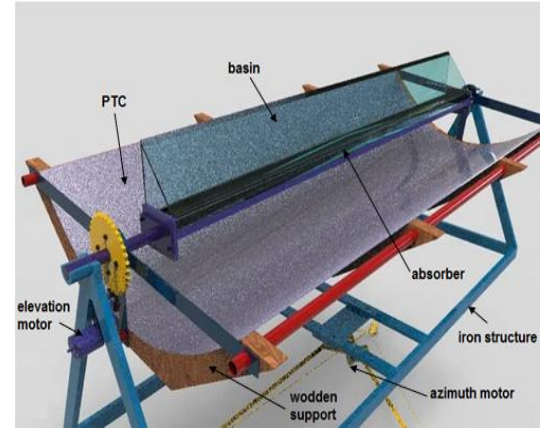


Fig. 2. Schematic view of parabolic trough concentrator conventional solar still (PTC-CSS)



Fig. 3. Pictorial view of parabolic trough concentrator conventional solar still

the predefined width of the commercial polished stainless steel. Thus, the focal length and the aperture diameter were considered respectively as 0.22 m and 0.88 m. The system design elements and their specifications are outlined in Table 1, while a schematic view and pictorial representation of the proposed solar still can be found in Fig. 2 and Fig. 3, respectively.

2.2. Experimental configuration and Instrumentation

Experiments were conducted during typical days in August on a conventional solar still integrated with a parabolic trough concentrator. The desalination unit was installed in the Energy and Farm Machinery Department, Hassan II Institute of Agronomy and Veterinary Medicine (Morocco), and was positioned at (33.97° N, -6.86° W). The measuring range was taken from 09:00h to 19:00h Morocco's official time zone. The atmospheric data was provided by a weather station type Davis Vantage Pro2 that was installed near the desalination unit. It registers permanently the values of radiation intensity, ambient temperature, and wind speed. The yield of distilled water was measured every 30 min by checking the level in the two graduated measuring jars placed on both ends of the solar still. Temperature data was recorded using four DS18B20 sensors inserted into different locations of the solar still. Table 2 presents the specifications of the instrumentation employed in the experimental setup, including the associated measurement uncertainties. The first DS18B20 sensor was attached to the absorber using a high-conductivity thermal paste to measure its temperature. The second one was placed on the inner surface of the absorber to measure the temperature of the shallow water. The third and fourth ones were used to measure the temperature of the vertical and condensing glass cover. Before integration into the experimental setup, all four temperature sensors DS18B20 were individually tested and calibrated using a thermostatic water bath. The sensors were immersed alongside a reference thermometer. Calibration points were taken at 5 °C intervals between 20 °C and 90 °C, covering the expected operating range. The readings from each sensor were compared with the reference, and linear correction factors were applied where necessary to ensure measurement precision. Sensors were linked to an Arduino MEGA2560 electronic board, which oversaw the system and stored the gathered data on an SD card.

In addition to data acquisition, the Arduino board also managed the sun-tracking system, which was implemented to optimize the concentrator's alignment with solar radiation

 Table 2

 Specifications of measurement instruments with associated uncertainties.

Instrument	Measurand	Accuracy	Range	Standard uncertainty
DS18B20	Temperature	±2 °C	-55°C to +125°C	1.155 °C
Davis vantage pro2	Temperature	±0.5°C	-40° to +65°C	0.288 °C
	Wind speed	±0.9 m/s	0 to 89 m/s	0.519 m/s
	Humidity	3%RH	1 to 100%RH	1.732 %RH
	Solar Radiation	5% of full scale	0 to 1800 W/m ²	51.961 W/m ²
Measuring jar	Yield	±10 ml	0–1500 ml	2.886 ml

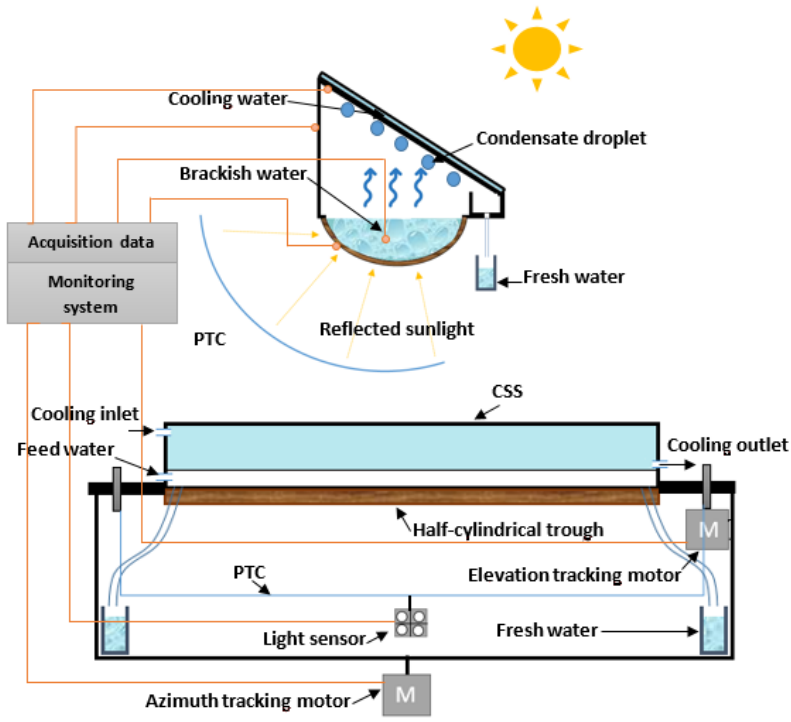


Fig. 4. Schematic of the experimental rig.

throughout the day. This automatic sun tracker controlled two 12 V direct current (DC) motors based on signals received from four light sensors. Two of these light sensors were used to detect the variation of the sun position with respect to the azimuth, while the two others were used to detect the elevation level. The first motor rotates the entire iron structure associating the concentrator with the basin, while the second motor turns only the parabolic concentrator around its focal line. The schematic of the experimental rig is provided in Fig. 4.

2.3. Cooling process

For comparative purposes, the initial experiment proceeded without the incorporation of any cooling method. Subsequently, two distinct experiments were carried out: the first involved directing water flow over the solar still top cover, while the

second entailed creating a glazed gap in the top cover and circulating water inside (condensing glass is submerged by cooling water). Details of the cooling parameters can be found in Table 3.

2.4. Solar still efficiency

Energy analysis for PTC-CSS is established according to equations given by Yılmaz and Mwesigye (2018). Power energy received by PTC is given as:

$$P = I_{(t)} \times A_p \tag{1}$$

Where A_p is the projected area of the PTC. Solar power energy reflected by PTC to the CSS is given as:

Table 3

Cooling parameters of PTC-CSS					
Cooling process	No cooling	Flowing over condensing glass cover	Submerging condensing glass cover surface		
Cooling fluid		water	water		
Cooling rate		1 cycle/ 30 min	1 cycle/ 30 min		
Condensing glass shape	simple	simple	Double glazed		
thickness	4 mm	4 mm	4mm/4 mm (5mm gap)		

$$P_r = P \times \cos\theta \times M_{ref} \tag{2}$$

Where θ is the angle of incidence and M_{ref} is the material reflectivity of the PTC.

The daily efficiency of the still, η_d , is obtained from the summation of the hourly condensate production during a day, m_{dist} , multiplied by the latent heat, h_{fg} ; the obtained result is divided by the total daily input energy plus the total energy consumed by the tracking system, $P_{\rm tracker}$, which is mainly due to the two motors, as shown in the following equation (Rahbar *et al.*, 2016).

$$\eta_{d} = \frac{\sum m_{dist} \times h_{fg}}{P_{r,daily} + P_{tracker}}$$
(3)

2.5. Uncertainty analysis

The error is the difference between the measured value and the true value of the measured quantity. There are two types of errors: (i) random error due to many factors such as hysteresis, parasites, environmental influences, etc... where we use generally statistical processing to know the most probable value of the measured quantity, and (ii) systematic error that superimposed on the random error and that will occur again with each measurement. It is caused, generally, by improper adjustment or calibration. Assessing uncertainty is equivalent to estimating the random error in a measurement. It gives access to an interval around the measured value where the true value is assumed to belong to. For a measuring device, it is common for the manufacturer to give its precision (a) without giving the law of error distribution. In this case, it is necessary to place oneself in the most unfavorable case and to consider that the density of probability is uniform in the interval [-a; +a]. Thus, the standard uncertainty can be estimated as (Modi et al., 2020):

$$\sigma_{x} = a/\sqrt{3} \tag{4}$$

For a graduated measuring device such as a rule or measuring tape using units such as inches or millimeters, the uncertainty is evaluated according to the minimum graduation of the device as (Ecole nationale superieure de chimie, n.d.):

$$\sigma_{x} = a/\sqrt{12} \tag{5}$$

When several independent variables $(x_1, x_2, ..., x_n)$ are measured to deduce the value of a quantity x, the uncertainty in each independent variable must be taken into account to calculate the uncertainty in this desired quantity. The uncertainty in the result σ_x could be calculated as follows (Hussein *et al.*, 2023):

$$\sigma_{x} = \sqrt{\left(\frac{\partial f}{\partial x_{1}}\right)^{2} \sigma_{x_{1}}^{2} + \left(\frac{\partial f}{\partial x_{2}}\right)^{2} \sigma_{x_{2}}^{2} + \dots + \left(\frac{\partial f}{\partial x_{n}}\right)^{2} \sigma_{x_{n}}^{2}}$$
 (6)

Water production and solar still efficiency are the most important parameters characterizing a solar still. Based on *Eq.* (3) and *Eq.* (6), the associated uncertainty with daily efficiency can be written as follows:

$$\sigma_{\eta} = \sqrt{\left(\frac{\partial \eta}{\partial m_{dist}}\right)^{2} \sigma_{m_{dist}}^{2} + \left(\frac{\partial \eta}{\partial I_{t,avrg}}\right)^{2} \sigma_{I_{t,avrg}}^{2}}$$
(7)

$$\sigma_{l_{t,avrg}} = \sqrt{\sum_{n=1}^{10} \left(\frac{\partial I_{t,avg}}{\partial I_{t,n}}\right)^2 \sigma_{l_{t,n}}^2}$$
(8)

$$I_{t,avrg} = \frac{1}{10} \sum_{n=1}^{10} I_{t,n} \tag{9}$$

Where It_{avrg} is the average daily solar radiation and It_n is the solar radiation in each measurement (n=1..10)

By the end of the experiment, we read one time the value of the total water yield from the two identical graduated bottles used by the system to collect distilled water.

$$m_{dist} = m_{dist1} + m_{dist2} \tag{10}$$

$$\sigma_{m_{dist}} = \sqrt{\left(\frac{\partial m_{dist}}{\partial m_{dist1}}\right)^2 \sigma_{m_{dist1}}^2 + \left(\frac{\partial m_{dist}}{\partial m_{dist2}}\right)^2 \sigma_{m_{dist2}}^2}$$
(11)

$$\sigma_{m_{dist}} = \sqrt{\left(\sigma_{m_{dist1}}\right)^2 + \left(\sigma_{m_{dist2}}\right)^2} \tag{12}$$

Also, in each measurement of solar radiation, the used device gives values with the same uncertainty. Basing on eq.(8) and eq.(9), we have:

$$\sigma_{l_{t,avrg}} = \sqrt{\sum_{n=1}^{10} \left(\frac{\sigma_{l_t}}{10}\right)^2}$$
 (13)

Then:

$$\sigma_{\eta} = \frac{\left(\frac{h_{fg}}{A_{p}\cos\theta M_{ref}l_{t,avrg}}\right)^{2}\sigma_{m_{dist}}^{2} + \left(\frac{-m_{dist}h_{fg}}{A_{p}\cos\theta M_{ref}(l_{t,avrg})^{2}}\right)^{2}\sigma_{l_{t,avrg}}^{2}}$$

Calculations showed that uncertainties associated with daily yield and average solar radiation measurements are 4.08 ml, and 16.43 W/m2 respectively, while the uncertainty related to the solar still efficiency was found to be <1%.

2.6. Economic study

In economic analyses pertaining to desalination units, the primary metric often considered is the CPL (Cost per Liter) of distilled water. It is determined by dividing the total annual cost of the system (TAC) by the annual yield of the solar still (M). On his part, the total annual cost of the solar still depends on the annual first cost (AFC), annual maintenance cost (AMC), and annual salvage value (ASV). It is mathematically expressed as (Mukherjee & Tiwari, 1986):

$$TAC = AFC + AMC - ASV \tag{15}$$

Where:

AFC= Initial investment (INV) × capital recovery factor (CRF) (16)

AMC = 15% of Annual first cost (17)

ASV = 10% of initial investment × Sinking fund factor (SFF) (18)

Where, *CRF* and *SFF* are functions dependent on the annual interest rate and the number of years the system will operate, they are formulated as:

$$CRF = \frac{ir \times (1 + ir)^n}{(1 + ir)^n - 1}$$
 (19)

$$SFF = \frac{ir}{(1+ir)^n - 1} \tag{20}$$

The payback period stands as another important metric in assessing the financial viability of desalination units. It evaluates the time needed for an investment to generate enough cash flow to recover its initial cost. the estimation of payback period can be expressed as (Ranjan & Kaushik, 2014):

$$p = \frac{\ln\left(\frac{CF}{CF - (INV * ir)}\right)}{\ln(1 + ir)}$$
(21)

where CF represents the cash flow, it is determined by multiplying the selling price of distilled water per liter by the yearly yield (M).

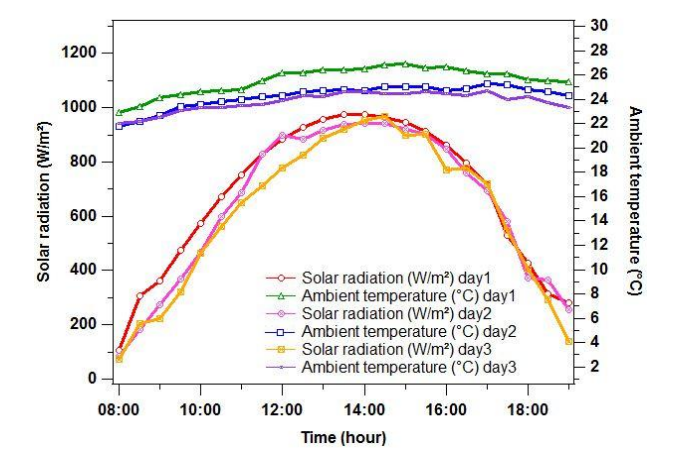
3. Results and Discussion

3.1. Experimental results

In this work, a conventional solar still was integrated with a parabolic trough concentrator. The desalination unit was equipped with a two axes solar tracker and the tests were carried out under the weather conditions of the city of Rabat, which is characterized by a semi-arid Mediterranean type climate with maritime or continental oceanic influence: mild, moderate and rainy in winter; and humid and temperate in summer. As depicted in Fig. 5, the ambient temperature during the three experimental days exhibited a typical diurnal pattern, progressively increasing in the morning hours, reaching a peak between 13:00 and 14:30, and then gradually declining toward the evening. Throughout the observation period, the ambient temperature remained below 27°C, with daily maximum values ranging between 24°C and 26.5°C depending on the day. The daily average wind speed during the experimentation of the PTC-CSS is recorded in the range from 4.52 to 4.57 m/s. In parallel, the wind speed showed a noticeable variation across the three days. It increased from early morning, reaching maximum values in the early afternoon, followed by a decline in the late afternoon. The daily average wind speed during the experimentation of the PTC-CSS ranged between 4.52 and 4.57 m/s. The highest wind speeds were recorded on Day 2, with peaks approaching 5.8 m/s around 14:00. These meteorological conditions—moderate ambient temperatures, sufficient solar radiation, and steady wind speeds—are favorable for evaluating the performance of thermally driven systems like the PTC-CSS. The relatively small variations in environmental parameters over the three days provide quasi-stable natural conditions, ensuring meaningful and comparable assessments of system behavior and efficiency. All experiments were performed with a starting amount of salt water of 2.5 liters. Refilling is facilitated via a slender conduit, directing it towards the inner surface of the absorber, prior to complete evaporation of water within the still. Details of the experiments cooling processes are shown in Table 3.

3.1.1. Case (I): No cooling

The experiment was conducted during a clear summer day of August 28th, 2022 without cooling the top cover surface. Fig. 5 shows the variation in ambient temperature, solar radiation and wind speed. It can be observed that the maximum-recorded



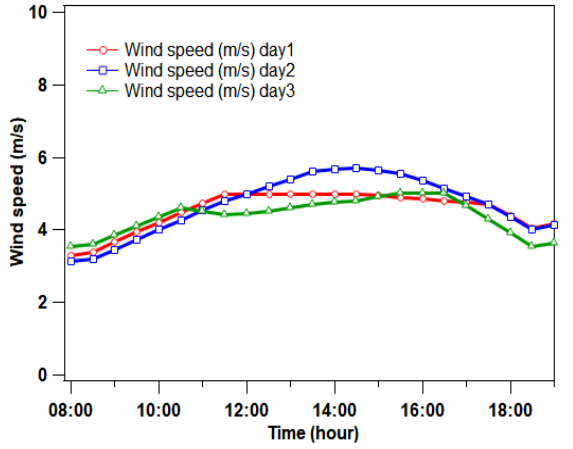


Fig. 5. (a) Variation of ambient temperature and solar radiation with respect to time. **(b)** Variation of wind velocity with respect to time.

ambient temperature is 26°C at 14:30, while the maximum value of solar radiation recorded is 974 W/m² at 14:00.

Fig. 6 shows the hourly variations of absorber, water, vertical side of glass cover and condensation glass cover temperatures. The maximum experimental temperature of water reaches 73.19 °C at 10:59, while the maximum experimental temperature of absorber is 75.14 °C at 11:44. It is observed that the temperature of the water reached the quasiready state quite rapidly due to the elevated temperature of the absorber and the limited water quantity within it. So, due to the effect of continuous concentration trained by PTC assisted solar tracker, the temperature curves of the studied system are different than normal conventional solar stills. For the latters, All curves begin to rise as solar radiation intensity expands, reaching their peak at noon, and subsequently tapering off thereafter. Solar still was refilled for the first time with an amount of saline water of 1 liter and then by 0.5 liters. The drop in water and absorber temperatures at 13:03 and 14:58 indicates the refill times. In addition to the temperatures of the water and absorber, temperatures of the glass cover are also seen to be affected when the absorber is refilled with warm saline water. This is due to the internal heat transfer processes that occurred within the basin. Water temperature was dependably higher than that of the glass cover. In a previous work conducted by Maliani et al. (2020), it was shown that heat and mass transfer processes that occur inside the PTC-CSS lead to an increase in the temperature of the glass cover by about 10°C lower than the water temperature. Vertical glass cover temperature was always lower than that of the condensation glass cover by 1°C to 2.5°C. In Fig. 6, it can also noticed that after reaching the steady-state,

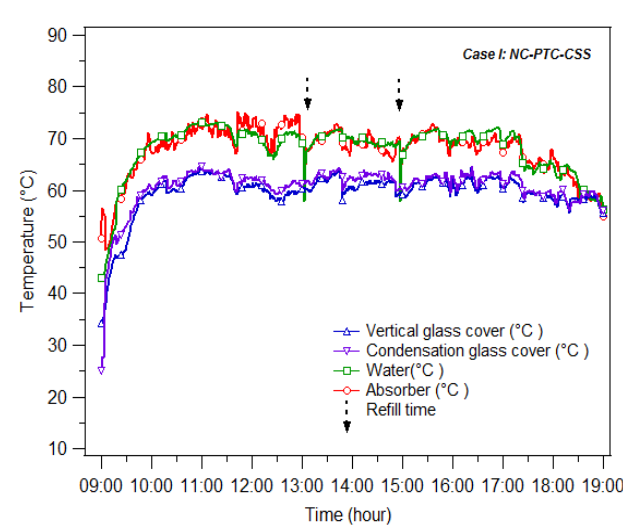


Fig. 6. Temperature variation of PTC-CSS with respect to time without cooling.

glass cover temperature kept a high value during most of the time of the experiment. At the end, both vertical and condensation glass cover still save a high temperature of 50°C. For many other solar stills operating under the same ambient temperature (Altarawneh *et al.*, 2017), this temperature value is never reached during any interval time of the experiment. The maximum value of ambient temperature was only 26 °C and it was reached at 14:30. However, the absorber kept a high temperature throughout experiment time intervals due to the effect of concentration. The cumulative productivity value of the system is illustrated in Fig. 12. Indeed, with an absorber area of 0.09 m² and an effective exploited collector area of 1.8 m² (CSS length is 1.8 m), 3.61 liters of distilled water were collected.

3.1.2. Case (II): water flow cooling

The second experiment was conducted on August 29th, 2022. In order to enhance the condensation rate of the solar still, a cooling process of the condensing glass cover was used by flowing water over the glass surface at a rate of 0.6 l every 30 minutes. Many small holes have been made in a plastic pipe by equal spacing to maintain a uniform flow over the condensing glass cover (Lawrence *et al.*, 1990). Fig. 7 represents the hourly

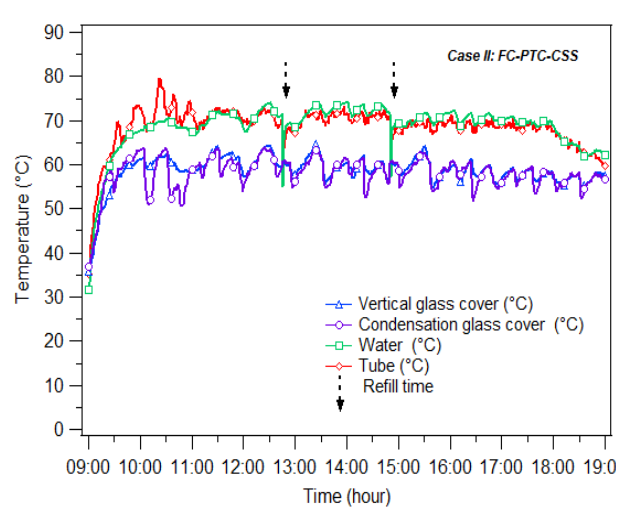


Fig. 7. Temperature variation of PTC-CSS with respect to time with cooling (water flow mode).

temperature variation of the absorber, water, vertical and condensing glass cover. Due to the effect of concentrator assisted solar tracker, all curves have a quasi-constant trend. During the experiment, some fluctuations in the temperature of the absorber were observed, attributed to imperfections in the automatic sun tracking system as it endeavored to align the concentrator's focal line with the absorber's position. Solar still was refilled two times by 1 liter and 0.5 liters at 12:46 and 14:51 respectively.

From Fig. 7, it was observed that water temperature governs all solar still curves. Water temperature varies throughout the day due to the radiation variation and the eventual water refilling action. The maximum water temperature observed was 74.06 °C and it is nearly the same compared to the first experiment. As water temperature inside the trough increases, it causes the heat of the humid air inside the still. This in its turn causes the increase of glass cover temperature. However, the cooling process used in the experiment affects only the inclined glass cover and not the vertical one.

To assess the impact of the cooling process used to reduce the glass cover temperature, a comparison of temperature distributions of the PTC-CSS with and without cooling was made (cases I and II). In this way and in order to eliminate the impact of temperature variation throughout the day, an interval time of 3 hours from 11:00 to 15:00 h was adopted in this study (Pal *et al.*, 2017). During this time interval, the solar still works under quasi-steady-state conditions since the variation of incident solar radiation remains slightly lower. Also, since it is not directly affected by the cold water flowing process, the temperature of the vertical side of glass cover was taken as a reference point of comparison with the temperature of condensing glass for both cases.

In Fig. 8 the temperature of condensing glass cover was compared with that of the vertical side of the glass cover. It was observed that the gap between the condensing cover and the vertical side is almost positive and it is about 0.40 °C when no cooling system was integrated with the solar still. However, the gap was almost negative and it is nearly 1.45 °C when the first cooling process was adopted. Hence, it can be concluded that flowing water over the top cover of the PTC-CSS has decreased the temperature of the glass cover by nearly 2°C.Fig. 12 presents the cumulative yield of the PTC-CSS in water flow

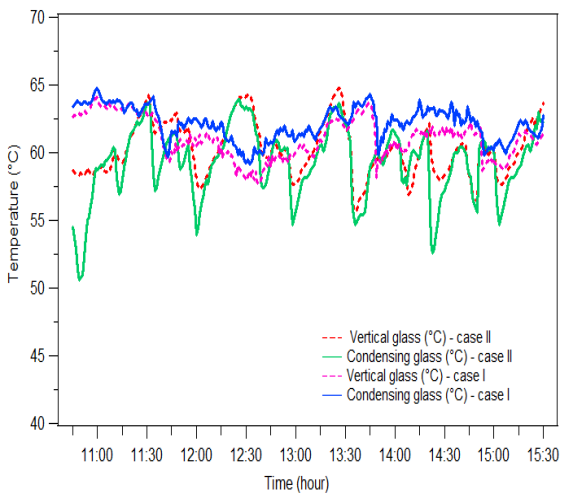


Fig. 8. Temperatures variation of vertical and condensation glass cover with and without cooling with respect to time.

cooling mode. The total distilled water produced was 4.05 liters. Compared with the still working with no cooling system, the yield has slightly increased. This can be attributed to the small contribution of the used cooling process to decrease the condensing glass temperature.

3.1.3. Case (III): cooling by submerging condensing glass

The experiment was carried out on a clear summer day, August 31st, 2022, with an initial volume of 2.5 liters of brackish water. The cooling process involves creating a glazing gap with the top cover and directing cooling water through it. Consequently, the initial condensing glass is submerged by cooling water. The gap is refilled with cooling water every 30 min and then evacuated. The modified basin of CSS described in Fig. 1-b above was used. Temperature distributions of the absorber, water and both vertical and condensing glass cover are shown in Fig. 9, while the variation of solar intensity and ambient temperature throughout the day are shown in Fig. 5-a. Water refilling was done three times at 12:45, 14:15 and 15:30. The maximum water temperature observed was 75.58°C and the minimum condensing glass cover and vertical glass cover observed in the quasi-ready state were 43.84 °C and 52.50 °C, respectively.

The temperature difference between water and glass cover was about (12-26) °C. Compared to a TSS working under the same conditions, this temperature difference is very advantageous. Elashmawyi (2019) has studied experimentally the cooling effect on a high standalone TSS. The two cooling techniques used, including that of passing cooling water inside 2mm between two concentric transparent tubes, were not able to increase the difference between water and glass cover. The results of his experiment showed that the difference never exceeded 3.5 °C. Moreover, the technique has a negative impact on productivity and has led to a significant decrease in water temperature. This was attributed to the fact that cooling water inside the two concentric glazed tubes lowers the transmittance value, and prevents solar radiation to reach water inside the absorber and, consequently, water productivity is decreased. On the other hand, before reaching the absorber, concentrated solar radiation needs to cross the two concentric tubes, causing the heat up of the water residing between them that, a priori, supposed to be a coolant fluid. This represents a second disadvantageous point.

Thus, in addition to the advantage of the compact design that allows easiness in matter of integration with a PTC, the

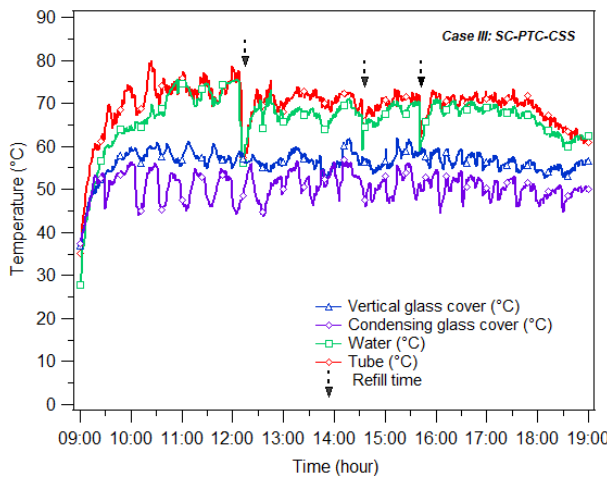


Fig. 9. Temperature variation of PTC-CSS with respect to time with cooling (submerging mode).

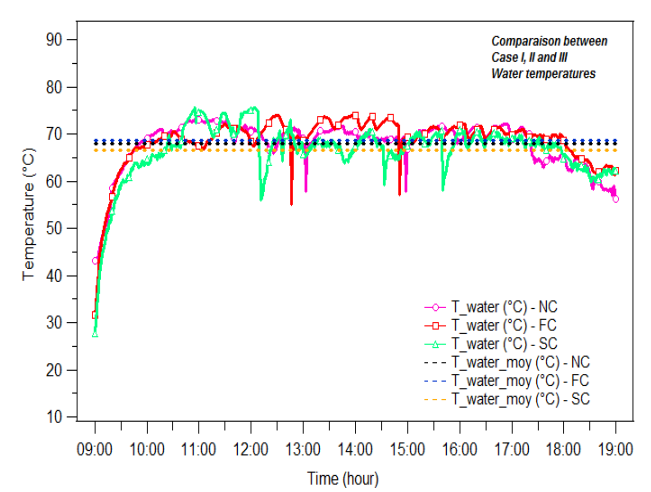


Fig. 10. Comparison of water temperature variation of PTC-CSS with respect to time in cases (I,II and III).

present CSS basin has overcome the previous constraints because the condensation cover is isolated from the absorber, and the concentrated solar radiation doesn't interfere with the condensation cover, nor with the cooling water. Consequently, this leads to a high driving force (T_w-T_g) of the solar still.

Fig. 10 gives a comparison between water temperature curves in the three cases of the experiment. It can be observed that there was no significant variation. The average water temperature values in these modes: no cooling mode, cooling by flowing water mode, and cooling by submerging the condensing glass mode were found to be nearly identical, in particular 68.62°C, 67.91°C, and 66.57°C, respectively. Compared to a TSS with concentric tubes for water-cooling coupled with a parabolic trough concentrator, the observed water temperature in case III is highly favorable as it remained unaffected. From the curves of the aforementioned study conducted by Elashmawyi (2019), it is evident that the same cooling process led to a decrease in water temperature by approximately 7 °C over large intervals of time during the experiment. The author has reported that this decrease was the primary reason for the decline in productivity and efficiency. The same remark was made by Lawrence et al. (1990) for a CSS with a water flow cooling surface.

Fig. 11 shows comparison curves of condensing glass cover temperatures for the three experiments. Due to the cooling processes conditions, an unstable behavior of the curves was observed in cases (II and III). The average temperatures of the condensing glass cover in the three cases were 60.55°C, 57.99°C, and 50.61°C, respectively. It can be remarked that the flow of water over the top cover of the PTC-CSS has reduced the glass cover temperature by nearly 2.5°C. When comparing this temperature difference with a CSS operating without a concentrator and under the same cooling mode, it can be observed that the difference is minimal. An experimental study conducted by Lawrence et al. (1990) has shown that the glass cover temperature is lowered by 15°C in comparison to that without water flow over the glass cover, which has led to an enhancement of solar still efficiency by 7%. Hence, it can be said that the effect of the first cooling process (case II) was not able to decrease intensively the temperature of the condensation cover of the PTC-CSS. This result could be attributed to the compact geometry of the basin. The same behavior could be remarked in experimental work conducted by Elashmawy (2019) on a TSS coupled with a PTC under a low cooling process consisting to spray water on the condensation surface. For a

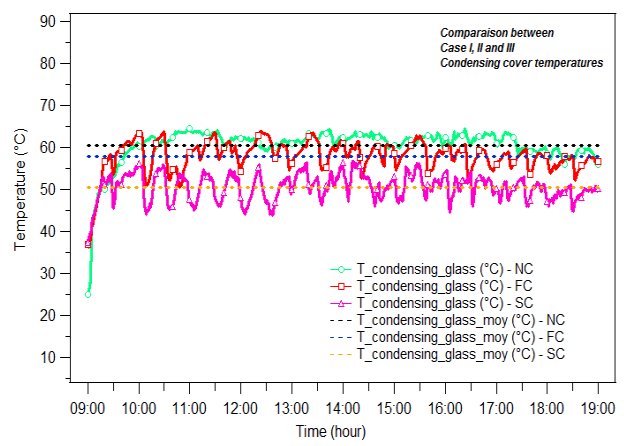


Fig. 11. Comparison of glass cover temperature variation of PTC-CSS with respect to time in cases (I, II and III).

large operating time interval, the temperature of condensing cover remained the same as when the still was working under no cooling mode. However, and as it can be seen from the curves of Fig. 11, the second cooling process has given a more satisfactory result. Passing cooling water through the glazed gap has led to a decrease in the condensing cover temperature by approximately 9.94°C compared to the first experiment and by about 7.37°C compared to the second one.

Also, in this aforementioned study performed by Elashmawy (2019), the author has reported that the two used cooling processes, either by spraying cold water or passing it between two concentric tubes, have had a negative impact on the productivity and the efficiency of the PTC-TSS, because of water temperature that was decreased when cooling water was covering the condensing tube surface. In this context and based on the curves given in Fig. 10, it can be observed that it was not the same situation for the PTC-CSS. The temperature of condensing glass cover was reduced and the water temperature inside the still was not considerably affected by the cooling process in both cases (II and III). This advantage was achieved through the design of the PTC-CSS, which was conceived in a way that the hot trough is separated from the condensing cover by an isolator and the predominant concentrated heat energy does not cross the condensing glass cover anymore.

To evaluate how the cooling method performs, we estimated the amount of heat absorbed by the stagnant cooling water layer placed between two glass panes. During repeated 30-minute cycles, the water was initially at a temperature ranging between 23 °C and 27 °C, depending on environmental conditions. The final water temperature recorded at the end of cycles varied between 42 °C and 60 °C. The contact surface area between the panes was $1.8 \text{ m} \times 0.15 \text{ m}$ (i.e., 0.27 m^2), and the cooling water layer had a thickness of 5 mm (0.005 m), corresponding to a volume of 0.00135 m3 and a mass of approximately 1.35 kg. The amount of heat absorbed by the water was calculated using the relation $Q=m\cdot c\cdot \Delta T$, where m is the mass of water, c is the specific heat capacity of water (4186 J/kg·°C), and ΔT is the temperature increase. Given the variation in final temperatures between 42 °C and 60 °C, the average final temperature is approximately 51 °C, resulting in a temperature difference of about 28-34 °C from the initial water temperature. The estimated heat absorbed over these cycles would thus be around 175-195 kJ, representing the average thermal energy extracted from the hot condensation glass cover during a 30-minute cooling cycle.

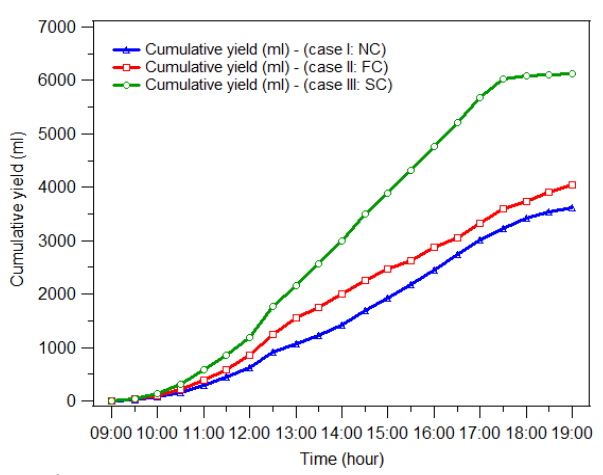


Fig. 12. variation of PTC-CSS yield with respect to time.

Fig. 12 presents the hourly variation of water productivity of the PTC-CSS for the three conducted experiments. The production rate depends on water, glass and atmospheric temperatures, as well as the temperature differences between water and glass, and between glass and the atmosphere (Kalidasa Murugavel et al., 2008). The PTC-CSS operates at high temperatures because of the continuous focus of the parabolic trough concentrator assisted solar tracker on the absorber's basin. The total daily productivity obtained without cooling (Case I) was 3611 ml/day. Flowing cool water on the top glass cover surface causes a positive effect on PTC-CSS productivity. The cumulative yield was determined to be 4050 ml/day, representing an improvement of 12.16% compared to the PTC-CSS operating in normal mode. The cooling technique of case II did not decrease considerably the temperature of the glass cover. Creating a glazed gap with the initial condensing glass cover and forcing cooling water to pass inside it has widened the water-glass temperature difference, which has improved the productivity. The yield was increased to 6120 ml/day, which is higher than the case I by 69.48%. In contrast, the PTC-TSS system with cooling water flowing between concentric tubes showed a 43.8% decrease in productivity (Elashmawy, 2019). Based on Eq.3, calculation results show that solar still efficiency in normal mode is 23.35%. The efficiency was increased when the first and second cooling modes were used to 26.20% and 39.59%, respectively. The two cooling techniques have experimented with only one flux rate. However, further studies aiming to choose the optimal flow mode of cooling water, namely, in function of various system temperatures are expected to give more satisfactory results.

3.2. Quality parameters analysis of PTC-CSS distilled water

Water quality parameters of PTC-CSS compared to the EPA standards for potable water were reported in Table 4. Three important parameters of two different samples including feed water and distilled water were measured in this context. The first parameter which is the pH. pH value gives an idea about the hydrogen ion concentration of a solution. The range of natural pH in fresh water extends from around 4.5 to over 10.0. However, the most frequently encountered range is 6.5-9.5 (Fri, 1972). pH value for both samples was found to be within the EPA acceptable range. Electrical conductivity was the second parameter that was measured. After distillation, the value of conductivity decreased remarkably. This indicates that an important amount of inorganic dissolved solids were removed

Table 4
PTC-CSS water quality results

PTC-CSS water quality results.						
parameters	Before	After	EPA std.			
	desalination	desalination				
pН	7.19	6.76	6.5-9.5			
TDS (mg/l)	3800	52	500			
Conductivity	5670	65	2500			
(µS/cm)						

from the feed water (EPA, 2012). It is often convenient to use electrical conductivity to give an estimation of the third parameter, TDS (total dissolved solids). Where TDS is high, the water may be saline and the obtained value of TDS was under permissible limits of EPA standard. So, the decrease in total dissolved solids (TDS) signifies the removal of ionized and non-ionized matter.

3.3. Cost analysis

A detailed assessment of the component costs is essential to understand the economic feasibility of the solar desalination system. Table 5 presents the cost of components within the desalination unit. The Parabolic Concentrator-Conventional

Solar Still system with cooling arrangement is priced at \$295. The solar still basin's costs \$77.89. The copper tube utilized in the construction of the solar still basin's incurs a cost of \$26.31 per meter length. To optimize the overall expense of the solar still, only half of the tube is utilized. Specifically, a copper tube of 0.9 meters is employed, and it is halved transversally. The two resulting portions are then seamlessly welded end to end to form the semi-cylindrical absorber measuring 1.8 meters. The tracking system costs \$137.89 and it stands out as the most expensive component, with a significantly higher cost compared to the other elements of the system. Priced at \$50.00, the cooling system is the least expensive yet has a positive impact. enhancing system efficiency and production without significant modification. Despite its lower cost, it plays a vital role in optimizing the overall performance of the solar distillation system.

In the current economic analysis of the solar still, it is assumed that the service life of the device and interest rate (ir) are 15 years and 12%, respectively. The total cost of the desalination unit is considered as the initial investment. Table 6 shows that for a conservative estimate, if the system works 300 days every year (65 days are assumed to be rainy or cloudy), average annual productivity varies significantly among cases, ranging from 1083 kg/year (Case II) to 1836 kg/year (Case III).

Table 5

Components' cost for the desalination uni

Component	Quantity	Cost/unit (MAD)	Cost
glass cover	lump sum	_	250 MAD (26.32 US\$)
copper tube	0.9 m	250 /m	225 MAD (23.68 US\$)
silicon sealant	1 unit	40 /u	40 MAD (4.21 US\$)
Total cost Solar still basin's			740 MAD (77.89 US\$)
polished stainless-steel sheet	2 m ²	$100 / m^2$	200 MAD (21.05 US\$)
wooden support	4 units	75 /u	300 MAD (31.58 US\$)
Total cost Parabolic Concentrator			500 MAD (52.63 US\$)
iron stand	lump sum	-	600 MAD (63,16 US\$)
DC motor 12V	2 units	200/u	400 MAD (42.11 US\$)
electronic circuit	1 card and 4 sensor	110/u	110 MAD (11.58 US\$)
battery	1 u	200 /u	200 MAD (21.05 US\$)
Total cost Tracking system			1310 MAD (137.89 US\$)
Water tank	1 u	100 /u	100 MAD (10.53 US\$)
iron support	1 u	150 /u	150 MAD (15.79 US\$)
pipes	lump sum	=	55 MAD (5.78 US\$)
labor cost, modification still basin's	lump sum	-	170 MAD (17.89 US\$)
Total cost Cooling system			475 MAD (50.00 US\$)
Total cost PTC-CSS with cooling a	rangement		2800 MAD (295 US\$)

1 US\$= 9.5 MAD

Table 6

Cost type	Case I	Case II	Case III	Unit
Total cost of still	245	272	295	US\$
AFC (annual first cost)	35.97	39.94	43.31	US\$
ASV (annual salvage value)	1.31	1.46	1.58	US\$
AMC (annual maintenance cost)	5.4	5.99	6.5	US\$
TAC (total annual cost)	40.06	44.47	48.23	US\$
M (average annual productivity) (yield *300 day)	1083	1215	1836	kg/year
CPL(cost of distilled water per liter)	0.037	0.0366	0.026	US\$
Efficiency	23.35%	26.20%	39.59%	%
Net profit	187.90	211.29	338.74	US\$/year
Payback period	1.3	1.29	0.87	year

Table 7

Design	Cooling System	Authors	Type of Concentrator and projected area	Basin evaporation surface	Yield	CPL (Cost Per Liter)	Total cost	Solar Tracking
CSS coupled with PTC	Water flow	Present study	PTC, 1.8 m ²	0.09 m ²	6.12 l/day	\$0.026	\$295	Automatic 2- axis
CSS coupled with PTC	No	(Maliani et al., 2020)	PTC, 1.8 m ²	0.09 m ²	3.76 l/day	\$0.038	\$245	Automatic 2-axis
TSS coupled with PTC	Water flow	(Elashmawy, 2019)	PTC, 0,87 m ²	0.078 m ²	2.10 l/day	\$0.035	\$192/m ²	Manual 2-axis
TSS coupled with PTC	No	(Elashmawy, 2019)	PTC, 0,87 m ²	0.078 m ²	3.71 l/day	\$0.015	\$150/m²	Manual 2-axis
Combination CSS - TSS coupled with CPC	Water flow	(Arunkumar et al., 2016)	CPC, 2 m ²	0.55 m ² (0.3 m ² + 0.25 m ²)	6.46 l/day	\$0.017	\$319	No
Combination Pyramid SS - TSS coupled with CPC	Water flow	(Arunkumar et al., 2016)	CPC, 2 m ²	1.3 m ² (0.3 m ² + 1 m ²)	7.77 l/day	\$0.016	\$359	No
TSS coupled with CPC	water flow	(Arunkumar et al., 2013)	CPC, 2 m ²	0.3 m ²	5.00 l/day	\$0.015	\$279	No

This increase in productivity is also associated with improved efficiency of the desalination unit in the two experiments where cooling techniques were implemented. Thus, the solar still's efficiency in the no cooling mode was only 23.35%. However, it increased to 26.20% and 39.59% when the first and second cooling modes were applied, respectively. The Cost per Liter (CPL) in Case III is significantly reduced to \$0.026, representing a substantial decrease of 29.7% compared to Case I (\$0,037) and 28.96% compared to Case II (\$0,0366). Considering \$0.21 as the average cost of distilled water in the local market, the annual profit for case III is calculated at \$338.74, resulting in a profit increase of 80.2% compared to Case I and 60.4% compared to Case II. Moreover, the payback period is remarkably shorter at 0.87 years, representing a reduction of 32.3% compared to Case I (1.29 years). The payback period remained relatively constant in Case II compared to Case I, which is attributed to the limited increase in productivity compared to the investment made. Thus, despite the elevated investment associated with the implementation of the cooling technique of Case III, it corresponds to significantly higher average annual productivity, lower cost per liter of distilled water, and improved profitability compared to the two other cases (Case I and II).

3.4. Comparison with solar desalination systems

Table 7 provides a comparison between the findings from the current study and relevant results obtained by other researchers working on solar stills coupled with concentrator. Economic analysis conducted on the present solar still without the integration of any water-cooling apparatus have shown that the cost per liter is approximately \$0.037. This result was obtained when an interest rate of 12% and a lifetime of 15 years with

around 300 operating days per year were considered. With the same assumptions, but an output of 6.12 L/day (case III), the CPL is approximately \$0.026. The total cost of the fabricated system with the water cooling arrangement would be approximately \$295. Therefore, although the use of water cooling system have increase the investment cost, the CPL was reduced by 29.73% due to the overall enhancement of water production. When conducting a comparative analysis between CSS and TSS, both integrated with PTC system, a notable discrepancy emerges in the influence of cooling apparatus on these two devices. Indeed, the utilization of a cooling mechanism enhances the yield of CSS, leading to a corresponding improvement in its Cost Per Liter (CPL). Conversely, the opposite outcome is observed for the TSS (Elashmawy, 2019). The use of combined systems, like the ones employed by Arunkumar et al. (2016), seems to be even more favorable in terms of Cost Per Liter (CPL). However, it can be remarked that this comes with a higher initial investment.

4. Conclusions

This study investigated the impact of condensing cover cooling on the performance of a dynamic conventional solar still (CSS) integrated with a parabolic trough concentrator (PTC) and assisted by a two-axis solar tracker. The system was designed to autonomously track the sun in both azimuth and elevation, ensuring continuous concentration of solar radiation on the absorber. Two cooling strategies were examined: the first involved circulating water over the condensing glass cover at a rate of 0.6 liters per 30 minutes, while the second consisted of submerging the entire condensing glass cover using a modified basin.

Experimental results revealed that surface cooling of the CSS had a positive impact on productivity, contrary to the TSS (Elashmawy, 2019), when both devices were associated with a PTC-assisted solar tracker. The highest yield, 6120 ml/day, was achieved when water was circulated through the double-glazing gap, followed by 4050 ml/day with flow over the condensing glass surface, and 3610 ml/day in no cooling mode. The driving force of the solar distillation technique (Tw - Tg) increased significantly when cooling water was forced to pass between the double-glazing glass cover, with the temperature difference reaching 10 °C. Compared to PTC-TSS (Elashmawy, 2019), the water temperature did not decrease when both cooling modes were applied, due to the PTC-CSS design, which benefits from concentrated heat radiation that does not need to cross the condensing cover before reaching the hot trough. Unlike PTC-TSS, the implementation of both cooling strategies in the PTC-CSS configuration heightened the temperature difference between the top cover and the basin water, thereby improving overall productivity.

Despite the implementation of cooling methods, the high temperature of the condensing glass cover remains a limiting factor in PTC-CSS systems. Nevertheless, both cooling approaches enhanced the thermal gradient across the system, thereby increasing overall productivity. The efficiency of the solar still improved from 23.35% in no cooling mode to 26.20% and 39.59% with the first and second cooling strategies, respectively. The cost per liter (CPL) was calculated to be \$0.026 and was reduced by 29.73% due to increased water output. Finally, water quality analyses confirmed that the distilled water met the standards set by the Environmental Protection Agency (EPA), indicating its suitability for safe consumption.

The cooling methods tested in this study have demonstrably enhanced the performance of the PTC-CSS, confirming their relevance for improving both distillate yield and still efficiency. Building upon these findings, future research could focus on the implementation of automated cooling systems using electric pumps, the investigation of optimal replacement rates for the cooling water, and the integration of thermal recovery by utilizing the warmed cooling water as preheated feed for the distillation process.

Nomenclature

Α	area	(m²)
---	------	------

a accuracy of the instrument

 h_{fg} latent heat of vaporization (J/kg)

intensity of solar radiation flux (W/m²)

m measured water yield (kg)

 M_{ref} materiel reflectivity

P Power (W)

t time (s)

T temperature (K)

Greek symbols

 θ angle of incidence (deg)

 η Efficiency (%)

uncertainty

Subscripts

avrg average
cond condensation
dist distilled
g glass cover

p parabola reflective surface

w water

Abbreviations

CSS conventional solar still

CPL cost per liter

PTC parabolic trough concentrator

SS solar still
TSS tubular solar still

Acknowledgments

We gratefully acknowledge Mr. Nabioui Said, a Mechanical Engineer and teacher at the National Education Ministry, for his invaluable support in 3D modeling using CAO/DAO software, as well as for his valuable recommendations and insightful opinions. We would also like to extend our heartfelt thanks to the mechanical workshop team of the Hassan II Institute of Agronomy and Veterinary Medicine, particularly Mr. Benhamad Bachir, for their outstanding technical assistance.

Statements & Declarations

Funding: The authors declare that no funds, grants, or other support were received during the preparation of this manuscript.

Competing Interests: The authors have no relevant financial or non-financial interests to disclose.

Ethics statement: This section may not be applicable.

Consent to participate: This section may not be applicable.

Data and material availability: The data that support the findings of this study are available from the corresponding author, O.D. Maliani, upon reasonable request.

Declaration of generative AI and AI-assisted technologies in the writing process

During the preparation of this work the authors used chatGPT 3.5 in order to improve readability and language. After using this tool, the authors reviewed and edited the content as needed and take full responsibility for the content of the publication.

References

Al-Madhhachi, H., & Min, G. (2017). Effective use of thermal energy at both hot and cold side of thermoelectric module for developing efficient thermoelectric water distillation system. *Energy Conversion and Management*, 133, 14–19. https://doi.org/10.1016/j.enconman.2016.11.055

Alrubaiea, J. F., Latteiff, F. A., Mahdi, J. M., Atiya, M. A., & Majdi, H. S. (2021). Desalination of agricultural wastewater by solar adsorption system: A numerical study. *International Journal of Renewable Energy Development*, 10(4), 901–910. https://doi.org/10.14710/IJRED.2021.38798

Altarawneh, I., Rawadieh, S., Batiha, M., & Mkhadmeh, L. (2017). Experimental and numerical performance analysis and optimization of single slope , double slope and pyramidal shaped solar stills. Desalination, 423, 124–134.

https://doi.org/10.1016/j.desal.2017.09.023

Arunkumar, T., Denkenberger, D., Velraj, R., Sathyamurthy, R., Tanaka, H., & Vinothkumar, K. (2015). Experimental study on a parabolic concentrator assisted solar desalting system. *Energy Conversion and Management*, 105, 665–674. https://doi.org/10.1016/j.enconman.2015.08.021

Arunkumar, T., Jayaprakash, R., Ahsan, A., Denkenberger, D., & Okundamiya, M. S. (2013). Effect of water and air flow on concentric tubular solar water desalting system. *Applied Energy*, *103*, 109–115. https://doi.org/10.1016/j.apenergy.2012.09.014

Arunkumar, T., Velraj, R., Denkenberger, D. C., Sathyamurthy, R., Kumar, K. V., & Ahsan, A. (2016). Productivity enhancements of compound parabolic concentrator tubular solar stills. *Renewable Energy*, 88, 391–400. https://doi.org/10.1016/j.renene.2015.11.051Ayoub, G. M., Malaeb, L., & Saikaly, P. E. (2013). Critical variables in the

- performance of a productivity-enhanced solar still. *Solar Energy*, 98(PC), 472–484. https://doi.org/10.1016/j.solener.2013.09.030
- Azari, P., Mirabdolah Lavasani, A., Rahbar, N., & Eftekhari Yazdi, M. (2021). Performance enhancement of a solar still using a V-groove solar air collector—experimental study with energy, exergy, enviroeconomic, and exergoeconomic analysis. *Environmental Science and Pollution Research*, 28(46), 65525–65548. https://doi.org/10.1007/s11356-021-15290-7
- Cuce, P. M., Cuce, E., & Tonyali, A. (2021). Performance analysis of a novel solar desalination system – Part 2: The unit with sensible energy storage with thermal insulation and cooling system. Sustainable Energy Technologies and Assessments, 48, 101674. https://doi.org/10.1016/j.seta.2021.101674
- Ecole nationale superieure de chimie. (n.d.). *Physique à l'ENSCR : erreur et incertitude*. Retrieved April 2, 2023, from https://physique.enscrennes.fr/erreur_incertitude.php
- Elashmawy, M. (2017). An experimental investigation of a parabolic concentrator solar tracking system integrated with a tubular solar still. *Desalination*, 411, 1–8. https://doi.org/10.1016/j.desal.2017.02.003
- Elashmawy, M. (2019). Effect of surface cooling and tube thickness on the performance of a high temperature standalone tubular solar still. Applied Thermal Engineering, 156, 276–286. https://doi.org/10.1016/j.applthermaleng.2019.04.068
- EPA. (2012). 5.9 Conductivity _ Monitoring & Assessment _ US EPA. https://archive.epa.gov/water/archive/web/html/vms59.html
- Fath, H. E. S., & Ghazy, A. (2002). Solar desalination using humidification-dehumidification technology. *Desalination*, 142(2), 119–133. https://doi.org/10.1016/S0011-9164(01)00431-3
- Fri, R. (1972). the Environmental Protection Agency1. *Journal of Milk and Food Technology*, *35*(12), 715–718. https://doi.org/10.4315/0022-2747-35.12.715
- Hafs, H., Ansari, O., & Bah, A. (2023). Impact of wind-driven mixed convection on the performance of passive solar desalination with PCM heat storage in varied Moroccan climates. *Acta Ecologica Sinica*. https://doi.org/10.1016/j.chnaes.2023.07.001
- He, T. xiang, & Yan, L. jun. (2009). Application of alternative energy integration technology in seawater desalination. *Desalination*, 249(1), 104–108. https://doi.org/10.1016/j.desal.2008.07.026
- Hussein, N. F., Ahmed, S. T., & Ekaid, A. L. (2023). Thermal Performance of Double Pass Solar Air Heater With Tubular Solar Absorber. *International Journal of Renewable Energy Development*, 12(1), 11–21. https://doi.org/10.14710/ijred.2023.46328
- Kalidasa Murugavel, K., Chockalingam, K. K. S. K., & Srithar, K. (2008). An experimental study on single basin double slope simulation solar still with thin layer of water in the basin. *Desalination*, 220(1–3), 687–693. https://doi.org/10.1016/j.desal.2007.01.063
- Kumar R, R., Pandey, A. K., Samykano, M., Aljafari, B., Ma, Z., Bhattacharyya, S., Goel, V., Ali, I., Kothari, R., & Tyagi, V. V. (2022). Phase change materials integrated solar desalination system: An innovative approach for sustainable and clean water production and storage. *Renewable and Sustainable Energy Reviews*, 165, 112611. https://doi.org/10.1016/j.rser.2022.112611
- Lawrence, S. A., Gupta, S. P., & Tiwari, G. N. (1990). Effect of heat capacity on the performance of solar still with water flow over the glass cover. *Energy Conversion and Management*, 30(3), 277–285. https://doi.org/10.1016/0196-8904(90)90010-V
- Le, T. H., Pham, M. T., Hadiyanto, H., Pham, V. V., & Hoang, A. T. (2021). Influence of various basin types on performance of passive solar still: A review. *International Journal of Renewable Energy Development*, 10(4), 789–802. https://doi.org/10.14710/IJRED.2021.38394
- Maliani, O. D., Bekkaoui, A., Baali, E. H., Guissi, K., El Fellah, Y., & Errais, R. (2020). Investigation on novel design of solar still coupled with two axis solar tracking system. Applied Thermal Engineering,

- 172, 115144. https://doi.org/10.1016/j.applthermaleng.2020.115144
- Modi, K. V., Nayi, K. H., & Sharma, S. S. (2020). Influence of water mass on the performance of spherical basin solar still integrated with parabolic reflector. *Groundwater for Sustainable Development*, 10(August 2019), 100299. https://doi.org/10.1016/j.gsd.2019.100299
- Morad, M. M., El-Maghawry, H. A. M., & Wasfy, K. I. (2015). Improving the double slope solar still performance by using flat-plate solar collector and cooling glass cover. *Desalination*, 373, 1–9. https://doi.org/10.1016/j.desal.2015.06.017
- Mukherjee, K., & Tiwari, G. N. (1986). Economic analyses of various designs of conventional solar stills. Energy Conversion and Management, 26(2), 155–157. https://doi.org/10.1016/0196-8904(86)90049-X
- Pal, P., Yadav, P., Dev, R., & Singh, D. (2017). Performance analysis of modified basin type double slope multi–wick solar still. *Desalination*, 422(April), 68–82. https://doi.org/10.1016/j.desal.2017.08.009
- Petersen, N. H., Arras, M., Wirsum, M., & Ma, L. (2024). Integration of large-scale heat pumps to assist sustainable water desalination and district cooling. *Energy*, 289, 129733. https://doi.org/10.1016/j.energy.2023.129733
- Prado, G. O., Gustavo, L., Vieira, M., Jorge, J., & Damasceno, R. (2016). Solar dish concentrator for desalting water. *Solar Energy*, *136*, 659–667. https://doi.org/10.1016/j.solener.2016.07.039
- Rahbar, N., Esfahani, J. A., & Asadi, A. (2016). An experimental investigation on productivity and performance of a new improved design portable asymmetrical solar still utilizing thermoelectric modules. *Energy Conversion and Management*, 118, 55–62. https://doi.org/10.1016/j.enconman.2016.03.052
- Rahmani, A., Boutriaa, A., & Hadef, A. (2015). An experimental approach to improve the basin type solar still using an integrated natural circulation loop. *Energy Conversion and Management*, *93*, 298–308. https://doi.org/10.1016/j.enconman.2015.01.026
- Ranjan, K. R., & Kaushik, S. C. (2014). Economic feasibility evaluation of solar distillation systems based on the equivalent cost of environmental degradation and high-grade energy savings. *International Journal of Low-Carbon Technologies*, 11(1), 8–15. https://doi.org/10.1093/ijlct/ctt048
- Shoeibi, S., Mirjalily, S. A. A., Kargarsharifabad, H., Panchal, H., & Dhivagar, R. (2022). Comparative study of double-slope solar still, hemispherical solar still, and tubular solar still using Al2O3/water film cooling: a numerical study and CO2 mitigation analysis. *Environmental Science and Pollution Research*, 29(43), 65370. https://doi.org/10.1007/s11356-022-20738-5
- Singh, D., Singh, S., Singh, D., Kushwaha, J., Mishra, V., Patel, S. K., Tewari, S., & Giri, B. S. (2024). Sustainable pathways for solar desalination using nanofluids: A critical review. *Environmental Research*, 241, 117654. https://doi.org/10.1016/j.envres.2023.117654
- Srithar, K., Rajaseenivasan, T., Karthik, N., Periyannan, M., & Gowtham, M. (2016). Stand alone triple basin solar desalination system with cover cooling and parabolic dish concentrator. *Renewable Energy*, 90, 157–165. https://doi.org/10.1016/j.renene.2015.12.063
- UN DESA. (2023). The Sustainable Development Goals Report 2023. In *The Sustainable development Goals Report 2023: Special Edition* (p. 80). https://unstats.un.org/sdgs/report/2023/
- Varun Raj, S., & Muthu Manokar, A. (2017). Design and Analysis of Solar Still. *Materials Today: Proceedings*, 4(8), 9179–9185. https://doi.org/10.1016/j.matpr.2017.07.275
- Yılmaz, İ. H., & Mwesigye, A. (2018). Modeling, simulation and performance analysis of parabolic trough solar collectors: A comprehensive review. *Applied Energy*, 225, 135–174 https://doi.org/10.1016/j.apenergy.2018.05.014



© 2025. The Author(s). This article is an open access article distributed under the terms and conditions of the Creative Commons Attribution-ShareAlike 4.0 (CC BY-SA) International License (http://creativecommons.org/licenses/by-sa/4.0/)